Surface XAFS – New Aspects of its Application in the Structural Study of Adsorption Phenomena

Haruo Kuroda[a] and Toshiaki Ohta[b]

[a]Research Institute for Science and Technology, The Science University of Tokyo, Noda, Yamazaki, Chiba 278, Japan, and [b]Department of Chemistry, School of Science, The University of Tokyo, Hongo, Bunkyo-ku, Tokyo 113, Japan

The use of surface XAFS for exploring new aspects of the structural study of the adsorption of atoms and molecules on solid surfaces is discussed. Three examples are considered: the chemisorption at step sites, the dynamical properties of the bonding between ad-atoms and substrates, and the adsorption of organic molecules on metal surfaces.

1. Introduction

The adsorption of atoms and molecules on metal surfaces has been extensively investigated by utilizing a variety of experimental techniques. Low-energy electron diffraction (LEED) has been successfully used in such studies to determine the structures of two-dimensionally ordered ad-layers formed on metal surfaces. However, when there is no long-range order related to the adsorption site, it is difficult to derive any structural information from LEED. On the other hand, X-ray absorption fine-structure (XAFS) spectroscopy can, by use of a surface-sensitive detection mode, 'surface XAFS', provide structural information irrespective of the presence of long-range order. Furthermore, since the adsorption state is less affected by X-ray irradiation, the surface XAFS technique can be applied not only for a strongly chemisorbed system but also in cases of molecular adsorption. In this sense, surface XAFS spectroscopy is complementary to LEED. In this article, we will consider a few examples illustrating new aspects of structural information that are obtainable by surface XAFS, primarily focusing on surface extended X-ray absorption fine structure (SEXAFS).

2. Chemisorption at step sites

As an example of a system in which only a very small number of atoms are adsorbed without long-range order, let us consider the adsorption of S atoms at the step sites of Ni(7 9 11) (Ishii et al., 1991; Ishii, 1993). At low coverage (0.08ML), the LEED pattern does not exhibit any new spots other than those characteristic of Ni(7 9 11). Thus, no information is obtainable by LEED about the S adsorption site. The S K-edge EXAFS were measured for X-ray polarization parallel and perpendicular to the step. An example of the observed spectra is shown in Fig. 1. The Fourier transforms of the EXAFS oscillations exhibit a predominant peak due to S–Ni(nearest) interaction. The S–Ni distance and the effective coordination number derived from curve-fitting analysis are listed in Table 1. On an Ni(7 9 11) stepped surface, there are six possible types of adsorption site, which are illustrated in Fig. 2. The effective coordination numbers estimated for these models are given in Table 1. We can see that the best agreement between observation and calculation regarding the effective coordination number ratios, $N^*(15°)/N^*(60°)$ and $N^*(15°)/N(60°)$, is found in the case of the step fourfold site. This result implies that, in the initial stage of the S adsorption, S atoms are preferentially adsorbed at the step fourfold site with an S–Ni distance of 2.27 (3) Å.

The adsorption sites of P and Cl atoms on an Ni(7 9 11) surface at very low coverage were also studied by the same technique (Konishi, Asakura, Namba, Kitajima & Kuroda, 1991; Ishii, Asakura, Ohta, Kitajima & Kuroda, 1993). It was concluded that P atoms were preferentially adsorbed at the step fourfold sites, whereas Cl atoms were mainly
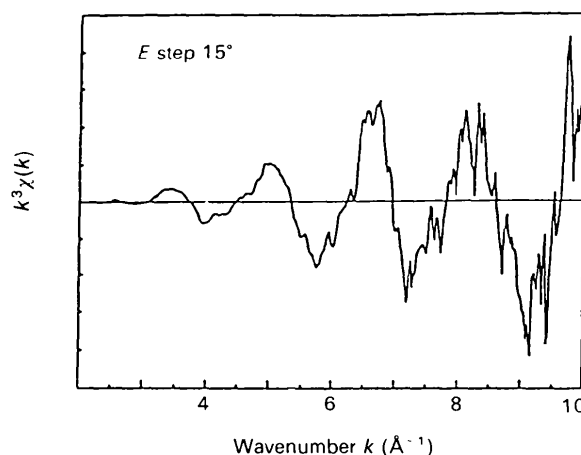

Figure 1
S K-edge EXAFS oscillation $k^3\chi(k)$ of S(0.08ML)/Ni(7 9 11), measured at glancing incidence ($\eta = 15°$, $E_\parallel$ step).

Table 1
Results of curve-fitting analysis of S K-edge EXAFS oscillation of
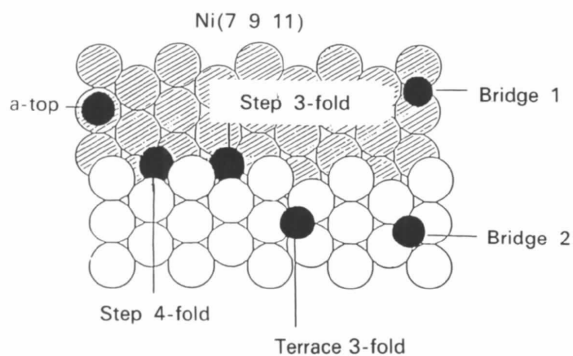S(0.08ML)/Ni(7 9 11).

	Observed		N^* (calculated)			
	R (Å)	N^*	Step fourfold	Step threefold	Terrace threefold	a-top
$E_\perp$ step						
15°	2.28	5.1	3.8	1.8	5.2	2.8
60°	2.28	5.0	3.7	2.8	2.7	0.75
90°	2.27	5.3	4.2	4.2	1.8	0
$N(15°)/N(60°)$	1.0		1.01	0.66	1.87	0
$N(90°)/N(60°)$	1.05		1.09	1.45	0.68	3.73
$E_{//}$ step						
15°	2.28	3.5	4.1	1.9	5.2	2.8
60°	2.26	4.2	4.0	2.0	2.7	0.75
90°	2.27	4.0	3.8	2.6	1.8	0
$N(15°)/N(60°)$	0.82		1.01	0.97	1.87	3.73
$N(90°)/N(60°)$	0.96		0.94	1.32	0.68	0

adsorbed at the terrace threefold sites. Seemingly, the dif-
ference of the adsorption behavior of Cl from those of S
and P is associated with the ionic character of the Cl–Ni
bond.

As demonstrated by the above examples, the SEXAFS
technique can provide structural information for the initial
stage of chemisorption. The detection limit of SEXAFS
will be further improved, even to trace amounts of adsorbed
atoms, by using a third-generation synchrotron radiation
source.

3. Dynamical properties of the bonding between ad-atom and substrate

Since the interatomic distances between an adsorbed atom
and the atoms of the substrate can be directly determined
by SEXAFS, the dynamical properties of these bonds can
be investigated from the temperature dependence of
EXAFS oscillation (Roubin et al., 1986; Wenzel, Stöhr,
Arvanitis & Baberschke, 1988; Lederer, Arvanitis, Comelli,
Tröger & Baberschke, 1994). To demonstrate the use of
this method, let us consider $c(2 \times 2)$S/Ni(100) and

$c(2 \times 2)$S/Ni(110) (Yokoyama *et al.*, 1994), whose struc-
tures are shown in Fig. 3.

Fig. 4 shows an example of the temperature dependence
of the Fourier-filtered EXAFS oscillations associated with
S–Ni interactions. Such data were analyzed by means of
'the ratio method'. Assuming the following anharmonic
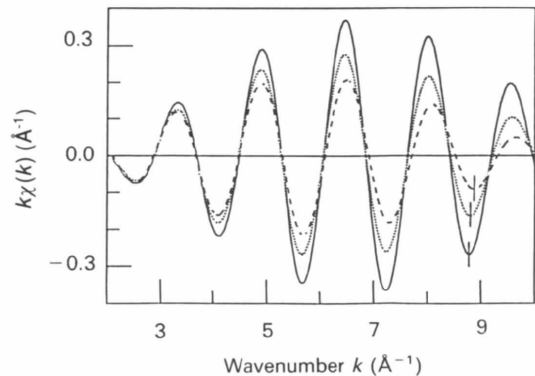potential function,

$$V(r) = (1/2)\alpha(r - r_0)^2 - \beta(r - r_0)^3,$$

the coefficients α and β and the equilibrium bond distance
r_0 in the above potential function, the Einstein temperature
Θ_E and the thermal expansion coefficient of bond length α_l
were determined for each Si–Ni bond. The results are sum-
marized in Table 2.

The dynamical properties of solid surfaces have been
investigated from the temperature dependence of LEED.
Such studies have revealed that surface phonons are gener-
ally much softer and more anharmonic in comparison with
bulk phonons. This phenomenon is considered to arise
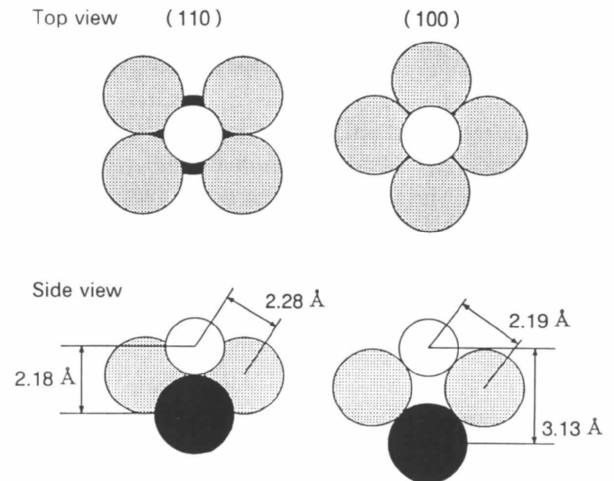
Figure 3
Structures of $c(2 \times 2)$S/Ni(110) and $c(2 \times 2)$S/Ni(100); open
circles = S, shaded circles = Ni(1) and solid circles = Ni(2).

Figure 2
Models of the adsorption sites on Ni(7 9 11). S atoms are selec-
tively adsorbed at the step fourfold site.

Figure 4
Temperature dependence of the Fourier-filtered $k\chi(k)$ function for
S–Ni of $c(2 \times 2)$S/Ni(110) at normal incidence. Solid, dotted and
dashed lines are the data at 100, 300 and 500 K, respectively.

Table 2

The dynamical properties of Si–Ni bonds derived from the temperature dependence of SEXAFS.

Bond	r_0 (Å)	α (eV Å^{-2})	β (eV Å^{-3})	Θ_E (K)	α_t (K^{-1})
S/Ni(100)					
S–Ni(1)	2.19	3.96	2.38	328	1.6 (3)
S–Ni(2)	3.13	1.52	0.88	203	3.0 (5)
S/Ni(110)					
S–Ni(1)	2.28	4.01	4.08	330	2.6 (5)
S–Ni(2)	2.18	5.49	1.61	386	0.5 (3)

mainly from the increase of the vertical thermal vibration of surface atoms. In the case of $c(2 \times 2)$S/Ni(100), the S–Ni(2) bond, which is vertical to the surface, is very much softer than the S–Ni(1) bond, as expected from the above-mentioned LEED studies. On the other hand, the situation was found to be contradictory in the case of $c(2 \times 2)$S/Ni(110), the vertical S–Ni(2) bond being very much tighter than the S–Ni(1) bond. Among the four S–Ni bonds studied here, the Einstein temperature is lowest for the S–Ni(2) bond of S/Ni(100), which has the longest inter-atomic distance, and highest for the S–Ni(2) bond of S/Ni(110), which has the shortest distance. This finding is consistent with the reported results of temperature-dependent SEXAFS studies on $p4g(2 \times 2)$N/Ni(100) and $(2 \times 2)R45$ 0/Cu(100) (Wenzel et al., 1988; Lederer et al., 1994). Seemingly, the dynamical properties of the bonding formed by an ad-atom are dependent mainly on the inter-atomic distance rather than the bonding direction. As demonstrated by the above example, the study of the temperature dependence of SEXAFS provides complementary information to that derivable from LEED.

4. Adsorption of organic molecules

Since X-ray irradiation has little effect on the chemical state of adsorbed species, surface XAFS is suited for the structural study of systems where organic molecules are adsorbed on solid surfaces. X-ray absorption near-edge structure (XANES) is known to exhibit a profile characteristic of a molecule. Thus, one can judge the chemical state of an adsorbed species from the observed XANES profile. The orientation of an adsorbed molecule can also be studied from the X-ray polarization dependence of XANES. An extensive review on this subject is given in the book by Stöhr (1992). However, it is difficult to determine the structural details solely from XANES data. Thus, it is important to combine XANES and EXAFS to perform a structural study. Let us now consider the adsorption of thiophenol on Ni(100) to illustrate the use of this approach (Takata et al., 1991).

A clean Ni(100) surface was dosed at 120 K with 1×10^{-4} Pa thiophenol (C_6H_5SH) for 3 min, and then the sample was heated to various temperatures for a short time. Fig. 5 shows the S K-edge XANES spectra measured at 120 K after the heat treatments. When the temperature

attained is in the region 127–176 K, the observed XANES profiles are almost the same as that of a condensed film of thiophenol, exhibiting little dependence on the direction of X-ray incidence. This fact indicates that a thiophenol multi-layer with random orientation of molecules remains on the surface. A significant change in XANES is observed when the treatment temperature is between 180 and 220 K. The XANES spectra are strongly dependent on both the incident angle and the polarization of the X-rays, exhibiting structures due to S–C and S–Ni bonds. The polarization dependence of XANES indicates that the S–C bond is nearly perpendicular to the Ni surface. On further elevating the treatment temperature above 220 K, the spectra gradually approach the S K-edge XANES of $c(2 \times 2)$S/Ni(100),
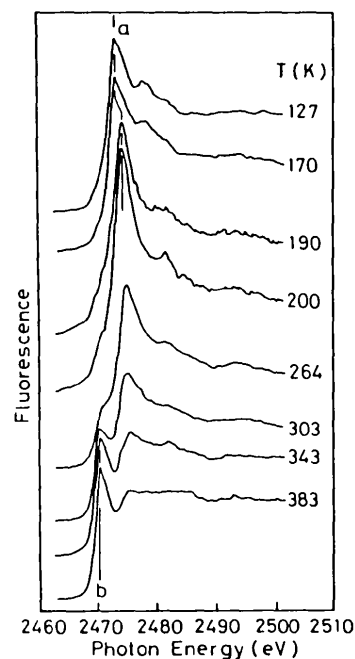

Figure 5
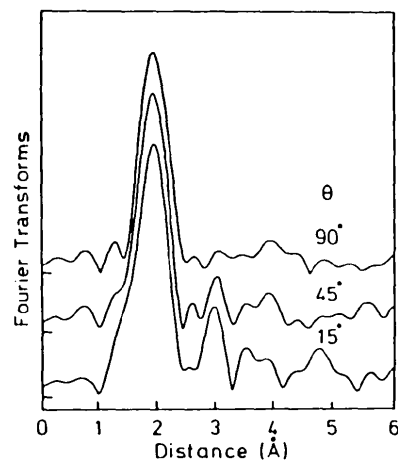S K-edge XANES of thiophenol/Ni(100) (at glancing incidence).

Figure 6
Fourier transforms of the S K-edge EXAFS oscillation $k^3\chi(k)$ after heating to 200 K.

suggesting cleavage of the S–C bond to yield S atoms chemisorbed at the fourfold hollow site of Ni(100).

Fig. 6 shows the Fourier transform of the S K-edge EXAFS oscillation observed for a sample heated to 200 K. The main peak in the Fourier transform of the glancing-angle incidence EXAFS data is asymmetric with a shoulder at about 1.4 Å, which is attributable to the S–C bond. By analyzing the main peak with the two-shell model, S–C and S–Ni distances were determined to be 1.84 and 2.24 Å, respectively. The polarization dependence of EXAFS indicates that the S–C bond is perpendicular to the Ni surface, in agreement with the conclusion from XANES. The curve-fitting analysis of the EXAFS oscillation due to S–Ni shows that the S atom is at the fourfold hollow site on Ni(100) with the S–Ni distance 2.25 (2) Å, this being almost the same as the chemisorption state of the S atom in $c(2 \times 2)$S/Ni(100). The derived structural model is illustrated in Fig. 7.

5. Summary and concluding remarks

In this article we have considered just a few examples to illustrate how and to what extent structural information concerning atoms or molecules adsorbed on solid surfaces can be derived from SEXAFS. We have tried to show the
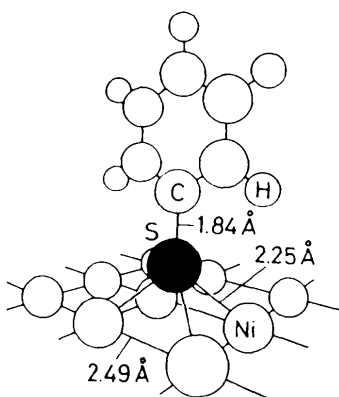
unique nature of SEXAFS spectroscopy as a tool for studying adsorption phenomena. If the number of adsorbed atoms or molecules is very low, as in the initial stages of adsorption, and the adsorption sites are randomly distributed over the substrate surface, LEED cannot provide any structural information. In such a case, SEXAFS is the only experimental technique that can be used to obtain direct structural information. For an ad-layer with two-dimensional order, LEED is the most powerful tool for determining the structure. However, even in such a case, SEXAFS can provide complementary information to that obtainable from LEED. In the last 10–15 years, applications of surface XAFS have developed at a considerable rate as pointed out by P. H. Citrin in his recent review of EXAFS and NEXAFS (Citrin, 1994). We can expect that the very much increased brightness of synchrotron radiation obtainable from a third-generation synchrotron radiation source will provide us with a chance to explore new applications of the surface XAFS technique.

Figure 7
Structural model for the chemisorption state of thiophenol on Ni(100).

References

Citrin, P. H. (1994). Surf. Sci. 229/300, 199–218.
Ishii, H. (1993). Thesis, Univ. of Tokyo, Japan.
Ishii, H., Asakura, K., Kitajima, Y., Funabshai, M., Namba, H., Kosugi, N., Ohta, T. & Kuroda, H. (1991). X-ray Absorption Fine Structure, edited by S. S. Hasnain, pp. 257–258. Chichester: Ellis Horwood.
Ishii, H., Asakura, K., Ohta, T., Kitajima, Y. & Kuroda, H. (1993). Jpn. J. Appl. Phys. 32(Suppl 2), 368–370.
Konishi, K., Asakura, K., Namba, H., Kitajima, Y. & Kuroda, H. (1991). Photon Fact. Act. Rep. 9, 213.
Lederer, T., Arvanitis, D., Comelli, G., Tröger, L. & Baberschke, K. (1994). Phys. Rev. In the press.
Roubin, P., Chandesris, D., Rossi, G., Lecante, J., Desjonqueres, M. C. & Treglia, G. (1986). Phys. Rev. Lett. 56, 1272–1275.
Stöhr, J. (1992). NEXAFS Spectroscopy, Springer Series in Surface Science, Vol. 25. Berlin: Springer-Verlag.
Takata, Y., Yokohama, Y., Yagi, S., Hoppo, N., Sato, H., Seki, K., Ohta, T., Kitajima, Y. & Kuroda, H. (1991). Surf. Sci. 259, 266.
Wenzel, L., Stöhr, J., Arvanitis, D. & Baberschke, K. (1988). Phys. Rev. Lett. 60, 2327–2390.
Yokoyama, T., Hamamatsu, H., Kitajima, Y., Takata, Y., Yagi, S. & Ohta, T. (1994). Surf. Sci. Submitted.